Effect of post-processing heat treatment on microstructure evolution and mechanical properties of in-situ Al/(Al₃Ni-TiC) hybrid composite fabricated by friction stir processing using mechanically activated powders

H. Fotoohi[1], B. Lotfi[1]*, Z. Sadeghian[1], J.-W. Byeon[2]

[1] *Department of Materials Science and Engineering, Faculty of Engineering, Shahid Chamran University of Ahvaz, Ahvaz 6135473337, Iran*
[2] *Department of Materials Science and Engineering, Seoul National University of Science and Technology, Seoul 01811, South Korea*

Abstract

Al matrix composites reinforced with in-situ synthesized TiC/Al₃Ni particles were fabricated by friction stir processing (FSP) using mechanically activated powders. The effects of post-processing heat treatment on the microstructure and mechanical properties were investigated. Ni-Ti-C powder mixtures were prepared by mechanical alloying (MA) and distributed in AA1050 alloy using FSP. The microstructure of composite layers was studied by optical and field emission scanning electron microscopy (FESEM), and structural evolutions during FSP and heat treatment were investigated by X-ray diffractometry (XRD). XRD analysis showed partial reaction between MAed powders and the matrix after 2 FSP passes and the formation of Al₃Ni and TiC compounds. Unreacted powders remained after 6 FSP passes, transformed to Ni₃Al and TiC after heat treatment at 550 °C. Mechanical properties of composite layers were investigated by tensile and microhardness tests. Heat-treated surface composite layer exhibited an increased tensile strength of 158 MPa with more uniform microhardness in comparison with the as-FSPed sample.

K e y   w o r d s: microstructure, particle reinforcement, hybrid composite, in-situ, FSP

1. Introduction

Al and its alloys are an important class of materials due to the combination of their low density and fairly good mechanical properties which make them suitable for a variety of applications. There has been a constant effort to improve the mechanical properties of Al alloys during recent decades. Al matrix composites have attracted considerable interest as high performance materials due to their high strength-to-weight ratio, stiffness, wear resistance, and high temperature stability compared to unreinforced alloys [1–5]. Therefore, they have been extensively used in defence, aircraft, aerospace, and automotive industries [6–8].

It is widely recognized that the mechanical properties of particulate-reinforced metal matrix composites (MMCs) are affected by the type of reinforced particles, particle distribution, and size and volume fraction of the reinforcements as well as the nature of the matrix/reinforcement interface. The interface between reinforcement and the matrix has been identified as a potential source of weakness in MMCs [9]. Thus, the mechanical properties of MMCs are very sensitive to the method of processing utilized [1, 10]. Several techniques have been employed to prepare the composites, including powder metallurgy and casting techniques [1-2].

In-situ MMCs in which the reinforcements are formed in the matrix through a reaction between elements or compounds have been developed in recent

decades. In-situ MMCs have exhibited many advantages compared to ex-situ MMCs, such as a clean reinforcement/matrix interface, thermodynamic stability and high bonding strength between the reinforcements and the matrix [10]. Many researchers have investigated the in-situ synthesis of intermetallic compounds (such as $NiAl_3$, $FeAl_3$, Al_3Ti, etc.) in Al matrix due to their high specific strength, high specific modulus, and excellent mechanical properties at both ambient and elevated temperatures [11–14]. Compared with the ex-situ method, in-situ synthesis has been shown to be suitable for the preparation of particulate-reinforced composites with remarkable improvements in mechanical properties [11]. Different processes such as mechanical alloying [15], powder metallurgy techniques [16], casting [17], and electromagnetic separation method [18] have been suggested for the fabrication of in-situ composites.

During recent decades, friction stir processing (FSP) as a severe plastic deformation process has been used by many researchers to fabricate MMCs. FSP was developed, based on the principles of friction stir welding (FSW), by Mishra et al. for microstructural modification of materials [19]. In this process, a rotating tool with a concentric shoulder and pin is plunged into the surface of a workpiece and revolved in the expected direction. The microstructure of the stirred zone is significantly refined and homogenized as a result of severe plastic deformation of material through stirring and thermal exposure resulting from friction between the tool and matrix. FSP has many applications such as the formation of ultrafine-grained structure in Al alloys [20, 21], microstructure homogenization in Al alloys fabricated by powder metallurgy [22], and improvement of the properties of cast Al alloys [23]. Furthermore, by adding second phase particles during FSP, surface composite layers can be formed on Al alloys [24, 25].

Very recently, a few studies have focused on the application of FSP in the in-situ fabrication of Al matrix composites. In these investigations, a very thin layer of reacted material has been reported to form on the surface of initial powder that makes a core-shell structure [26, 27]. However, a complete desired reaction between constituents has not been reported in previous works even after heat treatment [28].

The present study aimed to investigate the effects of post-heat treatment on the progression of in-situ reactions and properties of FSPed surface composite layer using reactive powders. The surface composite layer was fabricated on AA1050 substrate by FSP, with dispersing reactive Ti-Ni-C powders prepared by double stage mechanical alloying (MA). Structural evaluations were performed during FSP and after annealing using X-ray diffractometry (XRD). The distribution of particles in the matrix and mechanical properties of surface composite layers were studied.
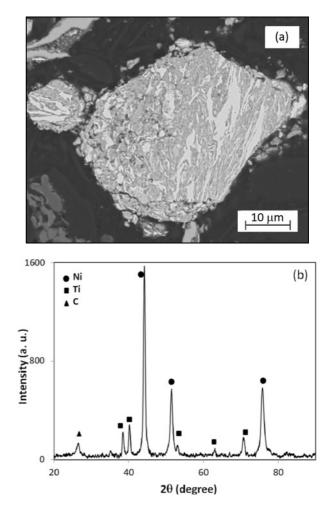

Fig. 1. (a) Cross-sectional SEM micrograph and (b) XRD pattern of Ni-Ti-C powder obtained from a total 10 h of double-step MA.

2. Materials and methods

Commercially available Ni (Merck, 99 %, $< 20\,\mu m$), Ti (Sigma-Aldrich, 99.9 %, 40–60 μm), and C (Merck, 99 %, $< 50\,\mu m$) powders were used as starting materials for powder preparation. Powder mixtures with a composition of Ni-32wt.%Ti-8wt.%C were milled using a planetary ball mill (Sepahan Equipment Company, Iran) similar to a Pulverisette 5 Fritsch. Chromium steel balls of 15 mm diameter with a ball-to-powder weight ratio of 10 : 1 were used as the grinding media. Hardened chromium steel vial was evacuated and filled with argon (99.99 %) to prevent oxidation during the MA process with a rotational speed of 600 rpm. The mentioned stoichiometric composition was tailored to achieve 50wt.%TiC with remained Ni to react with the Al matrix during FSP. Double stage MA was used to prevent self-propagating high-temperature synthesis (SHS) reaction during the MA process and formation of TiC during milling, according to a previous report [29]. In the first step, MA
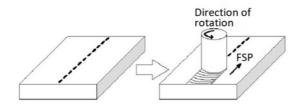
Fig. 2. Schematic illustration of the samples prepared for FSP of Al-Ni-Ti-C system.

was conducted on Ni-Ti and Ni-C powder mixtures separately for 5 h. Powders obtained in the first step were mixed and MA was repeated for 5 h in the second step to achieve a layered structure containing the initial constituents as shown in Fig. 1.

Commercially available pure Al (AA1050) was used as the substrate in the form of sheets of 10 mm thickness that were cut into 200 mm × 60 mm × 10 mm samples. Rank holes of 2 mm diameter and 3 mm depth were drilled in the surface of the specimens at 1 mm intervals. Ni-Ti-C powders obtained from a total 10 h of MA were placed into the rank holes as shown schematically in Fig. 2. FSP was performed using a hardened high carbon steel tool of 18 mm diameter and 5 mm length in the shoulder with a threaded cylindrical pin of 6 mm diameter and 5 mm length. Surface composite layers were prepared by 2, 4, and 6 FSP passes. A milling machine (X52, Machine Tool Works Co., Ltd.) was used to conduct the FSP experiments. The press-in depth of the tool shoulder into Al plate was set to 0.2 mm. FSP was conducted with a rotational tool speed of 1400 rpm and a traverse speed of 40 mm min^{-1} along the center line of drilled holes. Multi-pass FSP was applied in opposite directions to alter the retreating side and the advancing side in each pass when the workpiece was cooled to room temperature after the previous pass. FSPed samples were annealed at 550 °C for 4 h to study the influence of heat treatment on the microstructure of FSPed samples and investigate the possibility of in-situ reactions between unreacted MAed powders and the matrix during post-heat treatment.

Structural evolutions during MA and FSP and after annealing were investigated by using X-ray diffractometry with monochromatic CuK$_\alpha$ radiation (λ = 0.15406 nm). X-ray diffraction (XRD) scans were performed between 20° and 90° in 2θ with a step size of 0.05° and a dwell time of 10 s per step. Powder diffraction files (PDF) of the International Centre for Diffraction Data (ICDD) were used to identify the existing phases.

The microstructural examination was carried out on cross-sections of FSPed samples using an optical microscope (OM) (IM7200, Meiji Techno Co., Axbridge, England) and field emission scanning electron microscope (FESEM) (Mira 3-XMU). Powders were mounted in a conductive mounting resin and prepared by metallography techniques. Cross-sectional samples were polished using grinding paper up to 1200 grit followed by polishing using alumina suspension on polishing cloth for scanning electron microscopy (SEM). Energy dispersive spectroscopy (EDS) was used for elemental point analysis of specific phases.

To evaluate the hardness of FSPed samples, 100 g loading was applied for a dwell time of 10 s using a microhardness testing machine (Nexus Innova 4300). Hardness measurements were obtained along a line from FSPed layer to the base material to achieve hardness profiles. The mean value of three measurements was reported as the hardness of each point. Tensile test specimens were prepared according to the ASTM E8-M standard with a gauge length of 32 mm. Samples were cut from the stir zone of FSPed samples longitudinal to the center line using a wire cut machine. Tensile tests were carried out with a strain rate of 10^{-3} s^{-1} on at least three samples.

3. Results and discussion

3.1. Microstructural characterization

Figure 3 shows the typical optical macrographs of the stir zone of FSPed samples after 2, 4, and 6 passes. No macrostructural defect such as tunnels and wormholes can be observed in the stir zone of FSPed samples. Figure 3a depicts the non-uniform distribution of MAed powder particles in the Al matrix after 2 passes of FSP. This indicates that materials' flow and stirring action have not been adequate to distribute the particles after 2 FSP passes. Increasing the number of FSP passes to 4 resulted in a more uniform distribution of particles. After 6 FSP passes, a noticeable improvement in the microstructure with a more symmetric stir zone was observed (Fig. 3c). It is well understood that the rotating tool creates severe plastic deformation and the particles are distributed due to the thermo-mechanical effect and stirring of the matrix [19].

To investigate structural evolutions during the fabrication of surface composite layers, XRD analysis was performed on FSPed samples. XRD patterns of the FSPed surface composite layers obtained from different passes are presented in Fig. 4. Very weak peaks corresponding to Al$_3$Ni (ICDD PDF#00-002-0416) and TiC (ICDD PDF#00-006-0614) appeared in the XRD pattern after 2 passes of FSP.

According to thermodynamic data, different Ni-Al intermetallic compounds, namely, Ni$_3$Al, NiAl, Ni$_2$Al$_3$, and NiAl$_3$, exhibit negative free energy of formation [30]. Qian et al. have shown that for FSP conditions, the most negative effective free energy belongs to
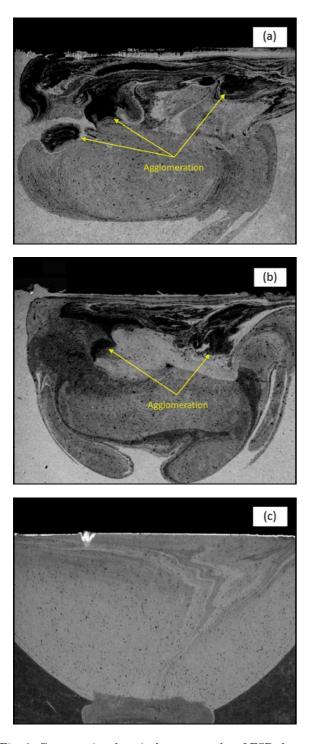
Fig. 3. Cross-sectional optical macrographs of FSPed surface composite layers after (a) 2, (b) 4, and (c) 6 FSP passes.

Fig. 4. XRD patterns of the surface composite layers obtained from different FSP passes.

NiAl$_3$ among different aluminides [31]. Moreover, the synthesis of TiC with a relatively large negative free energy of formation ($\Delta G_{f298} = -180.8\,\mathrm{kJ\,mol^{-1}}$) can be expected in the stir zone under FSP conditions [30]. After 4 and 6 FSP passes, the peaks corresponding to Al$_3$Ni and TiC show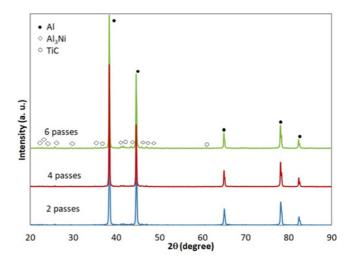ed a slight increase in intensity. By increasing the number of passes, the in-situ reaction has been promoted between Ni-Ti-C particles and the Al matrix. This can be interrelated to the increased interfaces in multi-layered structure powder and between the Al matrix and MAed particles as well as higher density of induced lattice defects as easy diffusion paths. The possibility of in-situ solid-state reactions in multi-layered mechanically alloyed powders has been established in many compositions [32].

Figure 5 shows the cross-sectional SEM micrographs of the surface composite layer obtained from 6 passes of FSP. Elongation and fragmentation of Ni-Ti-C particles in the Al matrix and distribution of fine in-situ synthesized particles can be seen in the micrographs. Higher magnification of the micrograph presented in Fig. 5b shows dark grey contrast particles distributed typically in the vicinity of the interface of Ni-Ti-C particles with the Al matrix (point A). These particles seem to be TiC as confirmed by the EDS analysis. As shown in Fig. 5a, a grey contrast layer (point B) can be found at the interface; this was shown to be Al$_3$Ni phase in EDS analysis, which is in agreement with the XRD results.

Simultaneous severe plastic deformation around the tool and friction between the tool and workpiece can generate localized heat in the stir zone. It has been reported that, during FSP, the maximum temperature in the stir zone of various Al alloys can be about 0.6 to 0.9 of melting point, depending on the process parameters [21]. It has also been stated that severe plastic deformation induced by FSP not only promotes mixing but also increases the diffusion rate of elements by heat and structural defects generation [32]. During the FSP of Al with Ni-Ti-C particles, the Al matrix is deformed and wrapped around the particles as a result of the stirring process and the particles
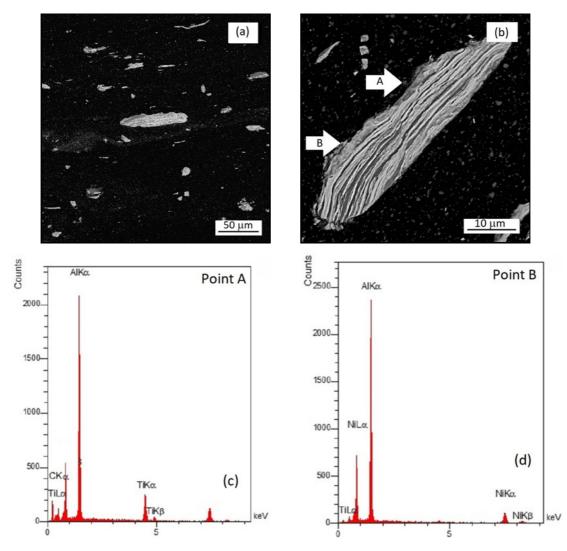
Fig 5. FESEM micrographs of surface composite layer obtained after 6 FSP passes: (a) distribution of particles, (b) an individual MAed particle at higher magnification, (c) and (d) EDS point analyses of depicted points.

are surrounded by the matrix that facilitates the reaction between Al and Ni. Brittle in-situ synthesized TiC and Al_3Ni compounds seem to break into smaller blocks and disperse in the matrix during FSP. Severe plastic deformation imposed by FSP can effectively remove in-situ synthesized products, and as a result, direct contact can be maintained between Al and unreacted Ni. Therefore, the reaction can continue at the interface, increasing the volume fraction of in-situ synthesized compounds.

Even after 6 FSP passes, some unreacted powder remained in the matrix. It has been reported in previous research that a considerable amount of unreacted Ni particles remained in the matrix after FSP of Al substrates with the addition of Ni particles [27, 28]. Previous researches have reported the formation of a core-shell structure around the induced particles with a thin intermetallic layer on the surface of particles. This has been attributed to the short duration of FSP at each pass [28]. However, a complete reaction may be
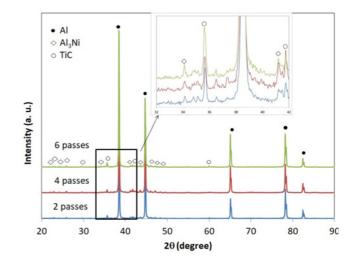

Fig. 6. XRD patterns of the surface composite layers obtained from different FSP passes after heat treatment at 550 °C.
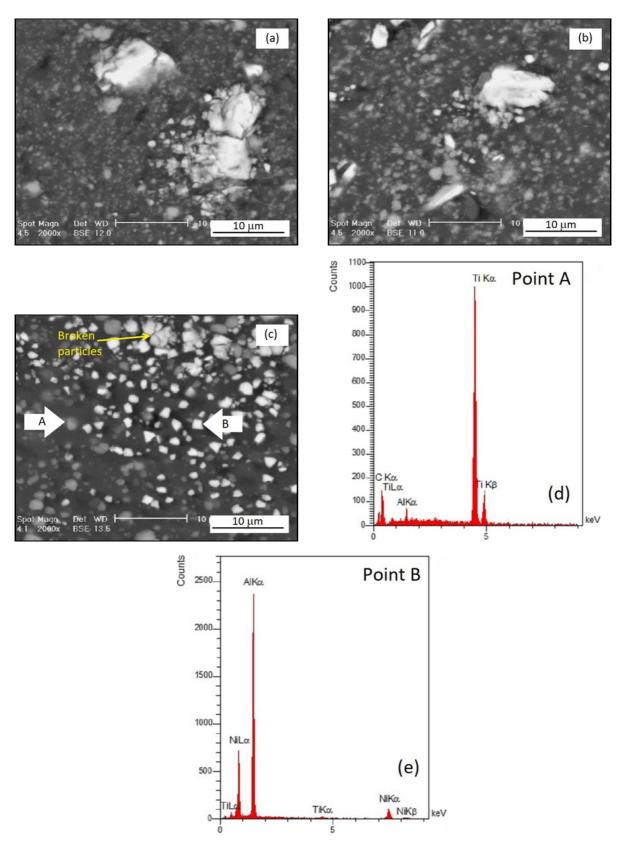
Fig. 7. Cross-sectional BSE micrographs of heat-treated FSPed surface composite layers obtained from (a) 2, (b) 4, (c) 6 FSP passes, (d) and (e) EDS point analyses of depicted points.

achieved by finer layers in the microstructure of MAed powders, which means shorter diffusion distances and more interfaces between the constituents.

Figure 6 shows the XRD patterns of FSPed samples after heat treatment at 550 °C. As can be seen, by increasing the number of FSP passes, stronger intensities of Al_3Ni and TiC peaks were obtained after annealing of the samples. The stronger intensity of these peaks can be considered as an evidence for increased formation of Al_3Ni and TiC. The peaks corresponding to TiC showed an apparent increase after heat treatment. High-temperature exposure seems to facilitate the diffusion of Ti and C atoms through the layers of MAed powder, resulting in a further reaction between elements.

Figure 7 shows the SEM micrographs of FSPed samples after heat treatment at 550 °C. Comparison of Figs. 5 and 7c shows the transformation of MAed powders after heat treatment. Instead of initial MAed powders, colonies of TiC and Al_3Ni particles can be seen in the matrix after 6 FSP passes, which are depicted concerning the EDS point analysis (Fig. 7d). However, even after heat treatment of the samples obtained from 2 and 4 FSP passes, a complete reaction between the elements in MAed particles and the matrix could not take place. As shown in Figs. 7a,b, some regions of MAed particles have remained unreacted after annealing heat treatment. Referring to XRD results, by increasing the FSP passes, an accelerated reaction can be expected during high-temperature exposure because of the increased diffusion paths in the matrix. In-situ formation of Al-Ni intermetallic compounds during heat treatment of Al/Ni diffusion couples has been investigated by several researchers [33–36]. It has been confirmed that the exothermic reaction between Al and Ni can proceed at about 550 °C [34]. The local temperature increase due to the exothermic reaction can trigger Ti/C in-situ reaction in MAed reactive powders, too. According to Bené's rule, the first phase that is formed during the interfacial reaction between two thin metallic films is neighboured to the low-temperature eutectic in the binary phase diagram, i.e., to Al in the present system, which is Al_3Ni [37]. Formation of intermetallic compounds induces a volume change between products and reactants which can result in interfacial stresses and formation of cracks. Consequently, reaction products can distribute in the ductile matrix by fragmentation of brittle products as well as individual nucleation. Fragmented and distributed particles can be seen in Fig. 7 and have been reported in previous studies, too [36, 38, 39].

It should also be noted that in all of the samples, porosities can be found in the vicinity of intermetallic particles. Considering the unbalanced solid-state diffusivity between Ni and Al, porosities may form due to the Kirkendall effect. Moreover, the volume change

Fig. 8. Microhardness profiles of the stir zone of the surface composite layers obtained from 2, 4, and 6 FSP passes compared to 2 passes FSPed AA1050 without powder addition.

between products and reactants can result in the formation of porosities [38]. Ke et al. reported an incomplete reaction between Ni particles and Al matrix even after heat treatment of FSPed samples at 550 °C [28]. Therefore, according to the results, it seems that with reactive powder prepared by mechanical alloying, which provides a thin-layered structure and induces a high density of lattice defects, in-situ reaction during heat treatment is facilitated.

3.2. Mechanical properties

Figure 8 shows the microhardness profiles of surface composite layers in comparison with the base AA1050 alloy after 2 FSP passes without the addition of powders. It should be mentioned that FSP without powder addition did not improve the microhardness, and the maximum value across the stir zone was about 40 HV, which is comparable with 34 HV of the as-received AA1050. However, a noticeable increase was observed in the average microhardness value in the stir zone of FSPed samples with Ni-Ti-C powder addition, which may be attributed to the in-situ synthesis of reinforcements. The maximum microhardness value after 2 FSP passes with Ni-Ti-C power was 140 HV. However, a non-uniform profile of the hardness was obtained across the stir zone of surface composite layer after 2 FSP passes, ranging from about 50 HV to about 140 HV. This can be explained by the non-uniform distribution of MAed particles, and consequently, in-situ synthesized compounds. In other words, some areas have been free from MAed powders, while, relatively high content of in-situ reinforcements have been formed in some other zones.
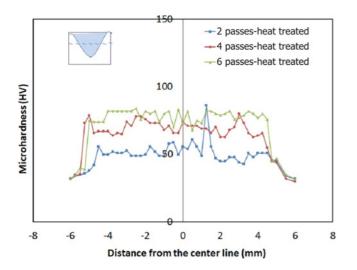
Fig. 9. Microhardness profiles of the stir zone of heat-treated surface composite layers obtained from 2, 4, and 6 FSP passes.

Mean hardness value increased with increase in FSP passes and reached 73 HV and 85 HV, respectively, after 4 and 6 passes of FSP with MAed powder. Such hardness increase can be directly attributed to the formation of fine Al_3Ni and TiC particles and their uniform dispersion in the Al matrix as indicated by XRD and SEM investigations. It is worth noting that the microhardness curves of FSP are uniform around the processing center line. It has been reported that grain size reduction with an increased number of FSP passes is not significant in Al [40]. Therefore, increased hardness can be mainly attributed to the formation of fine reinforcing particles and their uniform dispersion in pure Al matrix. As seen in Fig. 3, the agglomeration of reinforcing particles is apparent after 2 and 4 passes, and the particles have been more uniformly distributed in the matrix after 6 FSP passes.

Microhardness profiles of FSPed surface composite layers after heat treatment at 550 °C are shown in Fig. 9. Annealing has resulted in a slight increase in the hardness values of FSPed samples. However, by comparing the hardness profiles with those presented in Fig. 8, it can be concluded that after annealing treatment, more uniform hardness profiles have been obtained across the stir zone. Referring to SEM micrographs and XRD results, the transformation of MAed particles after high-temperature exposure can be considered as a reason for attaining the higher uniformity of hardness in surface composite layers. Shankar and Seigle [41] pointed out that the ratio of the intrinsic diffusivities of Ni and Al are strongly composition-dependent, and microstructural evidence has indicated that Al diffuses more rapidly than Ni in Al-rich alloys. Furthermore, investigation on the formation of $NiAl_3$ at the interface of Al/Ni bilayer showed that $NiAl_3$ grains protrude into the Al layer [42]. As seen in Fig. 7c, after heat treatment, MAed particles of layered structure (see Fig. 5) have transformed into individual particles, which were proved to be TiC and $NiAl_3$ particles according to EDS point analysis and XRD results. As it is evident in Fig. 7, in-situ synthesized TiC and $NiAl_3$ particles have been formed with individual nucleation and provided a fair distribution in the Al matrix.

Figure 10 shows the engineering stress-strain curves of surface composite layers obtained under different conditions in comparison with AA1050 base material. The highest ultimate tensile strength (158 MPa), which was obtained after heat treatment of the surface composite layer fabricated by 6 FSP passes, was about 188 % higher than that of the base material (84 MPa). It is worth noting that composite surface layers showed remarkably higher tensile strength in comparison with the as-received base material and FSPed AA1050. Ke et al. reported an ultimate tensile strength of 144 MPa during an attempt to fabricate
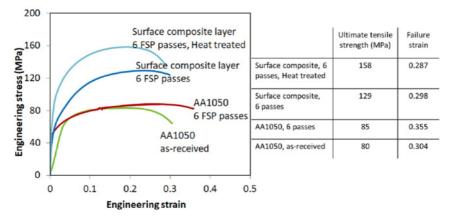

	Ultimate tensile strength (MPa)	Failure strain
Surface composite, 6 passes, Heat treated	158	0.287
Surface composite, 6 passes	129	0.298
AA1050, 6 passes	85	0.355
AA1050, as-received	80	0.304

Fig. 10. Engineering stress-strain curves of as-received AA1050, 6 passes FSPed AA1050, 6 passes FSPed Al-Al_3Ni/TiC and heat-treated 6 passes FSPed Al-Al_3Ni/TiC.
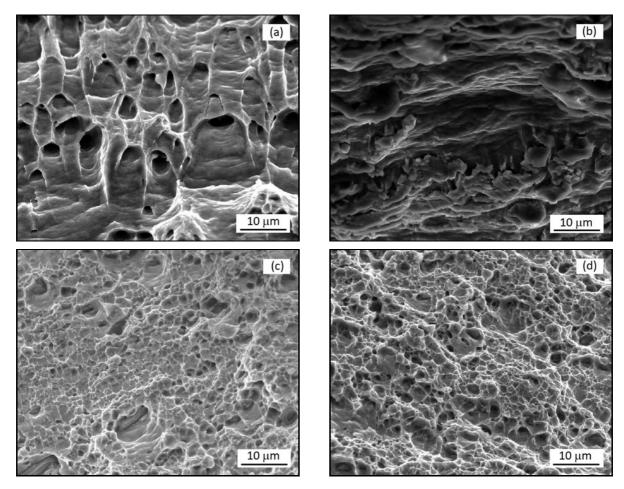
Fig. 11. SEM micrographs of fracture surfaces of (a) as-received AA1050, (b) 6 passes FSPed AA1050, (c) 6 passes FSPed Al-Al$_3$Ni/TiC, and (d) heat-treated 6 passes FSPed Al-Al$_3$Ni/TiC.

in-situ Al-Ni intermetallic composite through FSP. They reported incomplete reaction of Ni particles with the Al matrix [28]. Increasing of tensile strength and ductility of surface composite layers fabricated by FSP have been reported by several researchers [20, 22, 23, 41]. In-situ synthesized particles can result in grain refinement of FSPed composites via the Zener pinning effect which tends to improved ductility [12, 41]. Moreover, the enhancement of yield strength in surface composite layers, particularly after heat treatment, can be attributed to the Orowan strengthening mechanism inhibiting the dislocations from passing through the particles [43, 44]. The Orowan increment of yield strength of the in-situ Al-Al$_3$Ni/TiC composite obtained from post-heat treatment due to the second phase effect was calculated to be about 7 MPa according to the method presented by Kelly [45]. It should be mentioned that effects of particle size distribution, shape, and spacing that exist in a real material have not been considered in the equation. Moreover, the different thermal expansion coefficients of Al and reinforcing particles can create mismatch strains and increase the density of dislocations around the particles [43]. Shear-lag theory, which has

been explained as the mechanism of load transfer from the matrix to reinforcing particles using shear stresses at the interfaces between the composite components, may also lead to the higher strength of surface composites compared to unreinforced matrix [46]. According to the model discussed by Nardone and Prewo [47] the yield strength of in-situ matrix in the present study was predicted to increase by 1.085 times the yield strength of FSPed sample (62.7 MPa). Therefore, the yield strength of the composite by the shear-lag theory was estimated to be 68 MPa. The sum of Orowan and shear-lag effects gives the yield strength of 75 MPa which is in good agreement with the experimental offset yield strength of the sample obtained from post-heat treatment (78.3 MPa).

Figure 11 presents the SEM fractography of different samples after tensile experiments. On the fracture surface of AA1050 base material, relatively large equiaxed, shallow, and isolated dimples can be observed, which is the typical feature of ductile fracture. After 6 FSP passes on AA1050, elongated dimples appeared on the fracture surface and the flatness of the dimple network increased. This has been attributed to the high degree of plastic deformation induced by

FSP. In FSPed samples, failure occurs due to initiation of voids at triple junctions and sub-grain and/or grain boundaries.

Meanwhile, some voids may propagate through weaker paths, such as neighboring sub-grain and/or grain boundaries, and large dimples form by the coalescence of these voids [48]. The fracture surface of the in-situ surface composite layer obtained from 6 FSP passes shows dimples of various sizes (range: 1–10 μm). It should be noted that the average size of dimples decreased meaningfully in surface composite layers in comparison with the base material. Heat treatment of the FSPed surface composite layer resulted in a more uniform distribution of small dimples (Fig. 11d). This indicates the uniform distribution and good bonding of in-situ synthesized Al_3Ni and TiC particles with the matrix that facilitates effective load transfer.

4. Conclusions

Reactive Ni-Ti-C powder prepared through mechanical alloying was successfully incorporated into the Al matrix by FSP. Al_3Ni and TiC reinforcing particles were in-situ synthesized during FSP of Al with reactive powders. Increasing the number of FSP passes promoted the in-situ synthesis of reinforcing particles. In-situ synthesis of Al_3Ni and TiC reinforcements in the Al matrix resulted in increasing of the microhardness to 85 HV. Heat treatment of the surface composite layers obtained from 6 FSP passes provoked the reaction between remaining MAed powders and the matrix that resulted in more formation of TiC and Al_3Ni. In-situ synthesized surface composite layers obtained from 6 FSP passes showed 129 MPa tensile strength, which increased to 158 MPa after heat treatment.

Acknowledgements

References

[1] M. K. Surappa, Aluminium matrix composites: Challenges and opportunities, Sadhana 28 (2003) 319–334. doi:10.1007/BF02717141

[2] A. Ramanathan, P. K. Krishnan, R. Muraliraja, A review on the production of metal matrix composites through stir casting – Furnace design, properties, challenges, and research opportunities, Manuf. Process. 42 (2019) 213–245. doi:10.1016/j.jmapro.2019.04.017

[3] M. O. Bodunrin, K. K. Alaneme, L. H. Chown, Aluminium matrix hybrid composites: A review of reinforcement philosophies; mechanical, corrosion and tribological characteristics, Mater. Res. Technol. 4 (2015) 434–445. doi:10.1016/j.jmrt.2015.05.003

[4] L. Yuan, J. Han, J. Liu, Z. Jiang, Mechanical properties and tribological behavior of aluminum matrix composites reinforced with in-situ AlB_2 particles, Tribol. Int. 98 (2016) 41–47. doi:10.1016/j.triboint.2016.01.046

[5] H. Kwon, A. Kawasaki, M. Leparoux, Mechanical behaviour of dual nanoparticle-reinforced aluminium alloy matrix composite materials depending on milling time, Comp. Mater. 25 (2017) 3557–3562. doi:10.1177/0021998316673521

[6] D. K. Koli, G. Agnihotri, R. Purohit, Advanced aluminium matrix composites: The critical need of automotive and aerospace engineering fields, Mater. Today: Proc. 2 (2015) 3032–3041. doi:10.1016/j.matpr.2015.07.290

[7] S. T. Mavhungu, E. T. Akinlabi, M. A. Onitiri, F. M. Varachia, Aluminum matrix composites for industrial use: Advances and trends, Procedia Manufact. 7 (2017) 178–182. doi:10.1016/j.promfg.2016.12.045

[8] A. G. Arsha, E. Jayakumar, T. P. D. Rajan, V. Antony, B. C. Pai, Design and fabrication of functionally graded in-situ aluminium composites for automotive pistons, Mater. Des. 88 (2015) 1201–1209. doi:10.1016/j.matdes.2015.09.099

[9] G. Metcalfe (Ed.), Composite Materials: Interfaces in Metal Matrix Composites. Academic Press, New York, London, 2016. ISBN: 978-1-483-21667-6

[10] D. B. Miracle, Metal matrix composites – From science to technological significance, Compos. Sci. Technol. 65 (2005) 2526–2540. doi:10.1016/j.compscitech.2005.05.027

[11] S. C. Tjong, Z. Y. Ma, Microstructural and mechanical characteristics of in situ metal matrix composites, Mater. Sci. Eng. R 29 (2000) 49–113. doi:10.1016/S0927-796X(00)00024-3

[12] F. Adel Mehraban, F. Karimzadeh, M. H. Abbasi, Development of Al-Al_3Ni nanocomposite by duplex processing of flame spray and friction stir processing, and evaluation of its properties, Metall. Mat. Trans. A 48 (2017) 4693–4700. doi:10.1007/s11661-017-4273-9

[13] Y. Xue, R. Shen, S. Ni, D. Xiao, M. Song, Effects of sintering atmosphere on the mechanical properties of Al-Fe particle-reinforced Al-based composites, Mater. Eng. Perform. 24 (2015) 1890–1896. doi:10.1007/s11665-015-1470-9

[14] M. Yousefi, H. Doostmohammadi, Microstructure characterization and formation mechanism of functionally graded Al-$TiAl_3$ in situ composite by liquid-solid interaction, Alloys Comp. 766 (2018) 721–728. doi:10.1016/j.jallcom.2018.07.011

[15] V. A. Popov, E. V. Shelekhov, A. S. Prosviryakov, M. Y. Presniakov, B. R. Senatulin, A. D. Kotov, M. G. Khomutov, Particulate metal matrix composites development on the basis of in situ synthesis of TiC reinforcing nanoparticles during mechanical alloying, Alloys Compd. 707 (2017) 365–370. doi:10.1016/j.jallcom.2016.10.051

[16] O. Duygulu, High-resolution transmission electron microscopy investigation of in situ TiC/Al composites,

Kovove Mater. 56 (2018) 265–275.
doi:10.4149/km_2018_4_265

[17] N. Mathan Kumar, L. Annamalai Kumaraswamidhas, Characterization and tribological analysis on AA 6061 reinforced with AlN and ZrB_2 in situ composites, Mater. Res. Technol. 8 (2019) 969–980. doi:10.1016/j.jmrt.2018.07.008

[18] C. Song, Z. Xu, J. Li, In-situ Al/Al_3Ni functionally graded materials by electromagnetic separation method, Mater. Sci. Eng. A 445–446 (2007) 148–154. doi:10.1016/j.msea.2006.09.009

[19] R. S. Mishra, Z. Y. Ma, I. Charit, Friction stir processing: A novel technique for fabrication of surface composite, Mater. Sci. Eng. A 341 (2003) 307–310. doi:10.1016/S0921-5093(02)00199-5

[20] M. Regev, S. Spigarelli, Study of mechanical, microstructural and thermal stability properties of friction stir processed aluminum 2024-T3 alloy, Kovove Mater. 57 (2019) 229–236. doi:10.4149/km_2019_4_229

[21] F. Khodabakhshi, S. M. Arab, P. Švec, A. P. Gerlich, Fabrication of a new Al-Mg/graphene nanocomposite by multi-pass friction stir processing: Dispersion, microstructure, stability, and strengthening, Mater. Charact. 132 (2017) 92–107. doi:10.1016/j.matchar.2017.08.009

[22] Q. Zhang, B. L. Xiao, D. Wang, Z. Y. Ma, Formation mechanism of in situ Al_3Ti in Al matrix during hot pressing and subsequent friction stir processing, Mater. Chem. Phys. 130 (2011) 1109–1117. doi:10.1016/j.matchemphys.2011.08.042

[23] P. R. Guru, F. Khan, S. K. Panigrahi, G. D. Janaki Ram, Enhancing strength, ductility and machinability of an Al-Si cast alloy by friction stir processing, Manuf. Process. 18 (2015) 67–74. doi:10.1016/j.jmapro.2015.01.005

[24] N. Yuvaraj, S. Aravindan, V. Vipin, Fabrication of $Al5083/B_4C$ surface composite by friction stir processing and its tribological characterization, Mater. Res. Technol. 4 (2015) 398–410. doi:10.1016/j.jmrt.2015.02.006

[25] V. Sharma, U. Prakash, B. V. Manoj Kumar, Surface composites by friction stir processing: A review, Mater. Process. Technol. 224 (2015) 117–134. doi:10.1016/j.jmatprotec.2015.04.019

[26] G. Azimi-Roeen, S. F. Kashani-Bozorg, M. Nosko, P. Svec, Reactive mechanism and mechanical properties of in-situ hybrid nano-composites fabricated from an $Al-Fe_2O_3$ system by friction stir processing, Mater. Charact. 127 (2017) 279–287. doi:10.1016/j.matchar.2017.03.007

[27] I. S. Lee, P. W. Kao, N. J. Ho, Microstructure and mechanical properties of Al-Fe in situ nanocomposite produced by friction stir processing, Intermetallics 16 (2008) 1104–1108. doi:10.1016/j.intermet.2008.06.017

[28] L. Ke, Ch. Huang, L. Xing, K. Huang, Al-Ni intermetallic composites produced in situ by friction stir processing, Alloys Compd. 503 (2010) 494–499. doi:10.1016/j.jallcom.2010.05.040

[29] Z. Sadeghian, S. Zohari, B. Lotfi, C. Broekmann, Fabrication and characterization of reactive Ni-Ti-C powder by mechanical alloying, Alloys Compd. 589 (2014) 157–163. doi:10.1016/j.jallcom.2013.11.156

[30] I. Barin, Thermochemical data of pure substances. Wiley-VCH, Weinheim, 1989. ISBN: 3-527-27812-5.

[31] J. Qian, J. Li, J. Xiong, F. Zhang, In situ synthesizing Al_3Ni for fabrication of intermetallic-reinforced aluminum alloy composites by friction stir processing, Mater. Sci. Eng. A 550 (2012) 279–285. doi:10.1016/j.msea.2012.04.070

[32] C. Suryanarayana, Mechanical alloying and milling, Prog. Mater. Sci. 46 (2001) 1–184. doi:10.1016/S0079-6425(99)00010-9

[33] B. S. B. Reddy, K. Rajasekhar, M. Venu, J. J. S. Dilip, Siddhartha Das, Karabi Das, Mechanical activation-assisted solid-state combustion synthesis of in situ aluminum matrix hybrid (Al_3Ni/Al_2O_3) nanocomposites, Alloys Compd. 465 (2008) 97–105. doi:10.1016/j.jallcom.2007.10.098

[34] L. Battezzati, P. Pappalepore, F. Durbiano, I. Gallino, Solid state reactions in Al/Ni alternate foils induced by cold rolling and annealing, Acta Mater. 47 (1999) 1901–1914. doi:10.1016/S1359-6454(99)00040-3

[35] K. Morsi, Review: reaction synthesis processing of Ni-Al intermetallic materials, Mater. Sci. Eng. A 299 (2001) 1–15. doi:10.1016/S0921-5093(00)01407-6

[36] M. Rasouli, F. Akhlaghi, O. O. Ojo, M. Paidar, Preparation and characterization of in-situ $Al-Al_xNi_y$ composites via reactive infiltration, Alloys Compd. 780 (2019) 829–845. doi:10.1016/j.jallcom.2018.11.408

[37] R. W. Bené, First nucleation rule for solid-state nucleation in metal-metal thin-film systems, Appl. Phys. Lett. 41 (1982) 529–531. doi:10.1063/1.93578

[38] X. Chen, C. Li, S. Xu, Y. Hu, G. Ji, H. Wang, Microstructure and microhardness of $Ni/Al-TiB_2$ composite coatings prepared by cold spraying combined with post annealing treatment, Coatings 9 (2019) 565–585. doi:10.3390/coatings9090565

[39] C. R. Kao, J. Woodford, S. Kim, M. X. Zhang, Y. A. Chang, Synthesis of in situ composites through solid-state reactions: Thermodynamic, mass-balance and kinetic considerations, Mater. Sci. Eng. A 195 (1995) 29–37. doi:10.1016/0921-5093(94)06503-9

[40] D. Yadav, R. Bauri, N. Chawake, Fabrication of Al-Zn solid solution via friction stir processing, Mater. Charact. 136 (2018) 221–228. doi:10.1016/j.matchar.2017.12.022

[41] S. Shankar, L. L. Seigle, Interdiffusion and intrinsic diffusion in the NiAl (δ) phase of the Al-Ni system, Metall. Mat. Trans. A 9 (1978) 1467–1476. doi:10.1007/BF02661819

[42] E. Ma, M. A. Nicolet, M. Nathan, $NiAl_3$ formation in Al/Ni thin film bi-layers with and without contamination, Appl. Phys. 65 (1989) 2703–2710. doi:10.1063/1.342756

[43] N. Gangil, A. N. Siddiquee, S. Maheshwari, Aluminium based in-situ composite fabrication through friction stir processing: A review, Alloys Compd. 715 (2017) 91–104. doi:10.1016/j.jallcom.2017.04.309

[44] M. Karbalaei-Akbari, H. R. Baharvandi, K. Shirvani Moghaddam, Tensile and fracture behavior of nano/micro TiB_2 particle reinforced casting A356 aluminum alloy composites, Mater. Des. 66 (2015) 150–161. doi:10.1016/j.matdes.2014.10.048

[45] P. M. Kelly, Progress report on recent advances in physical metallurgy: (C) the quantitative relationship between microstructure and properties in two-phase alloys, Inter. Met. Reviews 18 (1973) 31–36. doi:10.1179/imtlr.1973.18.1.31

[46] X. N. Mu, H. N. Cai, H. M. Zhang, Interface evolution and superior tensile properties of multi-layer graphene reinforced pure Ti matrix composite, Mater. Des. 140 (2018) 431–441. doi:10.1016/j.matdes.2017.12.016

[47] V. C. Nardone, K. M. Prewo, On the strength of discontinuous silicon carbide reinforced aluminum composites, Scripta Met. 20 (1986) 43–48. doi:10.1016/0036-9748(86)90210-3

[48] K. Yang, W. Li, P. Niu, Cold sprayed AA2024/Al_2O_3 metal matrix composites improved by friction stir processing: Microstructure characterization, mechanical performance and strengthening mechanisms, Alloys Compd. 736 (2018) 115–12. doi:10.1016/j.jallcom.2017.11.132